THE JOURNAL OF PHYSICAL CHEMISTRY B

Article

pubs.acs.org/JPCB

Strategy of Directly Employing Paclitaxel To Construct Vesicles

Tao Sun,[†] Hui Yan,[‡] Guangcun Liu,[§] Jingcheng Hao,[†] Jie Su,[†] Shangyang Li,[†] Pengyao Xing,[†] and Aiyou Hao*[,†]

[†]School of Chemistry and Chemical Engineering, Key Laboratory of Colloid and Interface Chemistry of Ministry of Education, Shandong University, Jinan 250100, PR China

[‡]College of Chemistry and Chemical Engineering, Liaocheng Universtiy, Liaocheng 252000, PR China

[§]Qianfoshan Hospital Affiliated to Shandong University, Jinan 250018, PR China

Supporting Information

ABSTRACT: A class of aza-arm modified β-cyclodextrins were found to be able to trap paclitaxel (PTX), an effective but strongly hydrophobic anticancer drug, to form novel "supramolecular amphiphiles", which can further self-assemble into vesicular structures in aqueous solution. The obtained vesicles were characterized in detail by transmission electron microscopy (TEM), scanning electron microscopy (SEM), cryogenic transmission electron microscopy (cryo-TEM), and dynamic light scattering (DLS). The mechanism of the vesicular formation was suggested on the basis of the experimental results of nuclear magnetic resonance (NMR), Fourier transform infrared spectroscopy (FT-IR), X-ray diffraction (XRD), and thermal analysis. The effects to the vesicular formation by changing the host molecules and solvents were also studied. The vesicles will disappear upon the introduction of Cu^{2+} into the vesicular system, during the procedure of which, PTX will be released meanwhile. We believe that our research will provide a new strategy of directly employing special drugs to construct microvehicles to carry other targeted molecules.

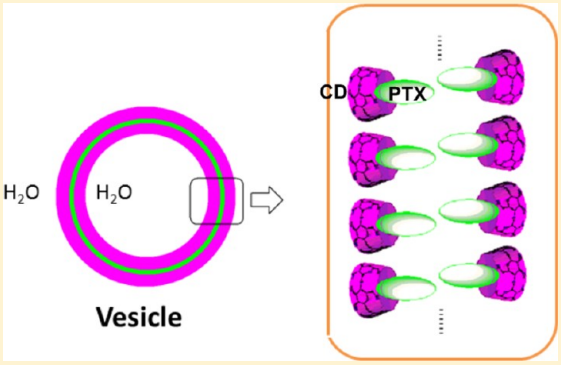

1. INTRODUCTION

Aggregates assembled by supramolecular amphiphiles have been thoroughly investigated as an effective means to obtain advanced responsive materials, including gels,[1] supramolecular polymers,[2] vesicles,[3−20] nanoscopic fibrils,[21] nanowires,[22] and functional rotaxane,[23] with the hope of practical applications in the fields of molecular machine, smart nanodevice and drug-carrier system. The supramolecular interactions (e.g., the inclusion phenomenon between the host and guest molecules) play a key role in linking the hydrophilic and hydrophobic moieties. Therefore, it is more promising in constructing stimuli-responsive materials with the "building blocks" of supramolecular amphiphiles. Vesicles, enclosing a volume with membranes consisting of bilayers or multilayers,[24] are always considered as efficient drug vehicles and one of the best models in mimicking the biomembranes. Vesicles self-assembled from supramolecular amphiphiles have correspondingly more potential in realizing the external-stimuli responsive functions, which are always regarded as favorable ways to mimic the biologic processes by chemical substrates as well as to achieve the controlled release of targeted drug.[25] Supramolecular amphiphiles can also additionally provide more opportunities in improving the properties of the aggregates by conveniently altering the guest and host molecules.[26] Many specially designed hydrophobic compounds (such as anthraquinone derivates,[3,4] ferrocene derivates,[5−11] azo-benzene compounds,[12−16] phthalate esters[17]) and even some common hydrophobic molecules without intentional modifications (such as ethyl benzoate,[18] bromophenol blue,[19] and methyl orange[20]) were reported to be capable of playing the role of hydrophobic tails to construct supramolecular amphiphiles. Thus, an idea came to us that if we directly employ some insoluble drug molecules as the hydrophobic tails to construct supramolecular amphiphiles as the building blocks for more advanced aggregates, the obtained aggregates themselves are solubilized drugs in natural and can probably act as the nanocarries for other aims.

PTX (Scheme 1), isolated from the bark of *Taxus brevifolia*, is a well-known and widely used anticancer agent, which can provide effective treatment for a wide range of carcinomas by interfering with microtubule breakdown during cell division.[27] However, the strong hydrophobicity of PTX has drastically limited its application in natural form. To date, some attempts have been made to solubilize PTX for better clinical effects.[28−30] However, complicated preparation procedures are still significant concerns for these sophisticated formulations. Therefore, an easy, effective and body-friendly system is highly

Received: October 17, 2012
Revised: November 29, 2012
Published: November 29, 2012

dx.doi.org/10.1021/jp310261j | J. Phys. Chem. B 2012, 116, 14628−14636

Scheme 1. Structures of PTX and ED-β-CD

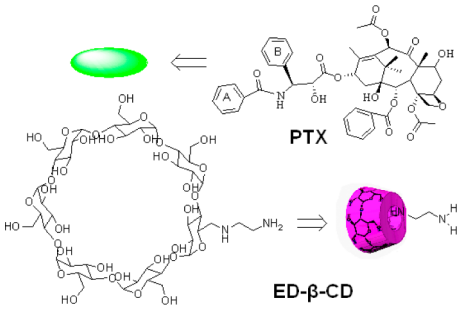

desirable on the way to translating this insoluble drug from bench to clinic.

We reported that if PTX was coated to vesicles with a size of about 200 nm, it would be easier to be up-taken by tumors, even with a better anticancer effect than the natural PTX dissolved in DMSO.[30] This may be due to the enhanced permeability and retention (EPR) effect.[31,32] PTX is extremely hydrophobic with the possibility of acting as the hydrophobic tails of the supramolecular amphiphiles for more advanced microarchitectures. The strategy will provide an exceedingly convenient way to produce microspheres loading with PTX and possible vehicles for other drugs.

On the basis of these considerations, cyclodextrin (cyclomaltoheptaose) seems to be a good choice for the biocompatible host molecules (also as the hydrophilic heads). Cyclodextrins, a series of α-1,4-linked cyclic oligosaccharides composed of 6, 7, or 8 D-(+)-glucose repeat units (corresponding to α-, β- and γ-cyclodextrins, respectively), are widely used as the host molecules in supramolecular chemistry for their low-cost, water-soluble, biocompatible, and easily modified properties.[33] More importantly, their proper hydrophobic cavities may provide proper shelters for certain guest molecules. Nanostructures based on cyclodextrins would combine the properties of molecular devices and macrocyclic host molecules together. Integrating cyclodextrin into vesicles may also bring about the supramolecular hosts' molecular recognition ability.

We attempted to employ different cyclodextrin derivates to include PTX with the hope of forming suitable supramolecular amphiphiles. The candidates of a class of mono aza-arm modified β-cyclodextrins were found to be able to include PTX to form corresponding supramolecular amphiphiles and further construct into vesicular spheres in the aqueous solution. The vesicles were fully characterized by TEM, SEM, cryo-TEM, and DLS means. The mechanism of the vesicle-formation was suggested on the basis of the ^{1}H NMR, 2D NMR ROESY, FT-IR, XRD, and thermal analysis results. The effects of the change of host molecules and the solvents to the vesicular formation were also studied. The vesicles will disappear upon the introduction of Cu^{2+} and release PTX at the mean time. We hope the research will introduce a new strategy of "directly using drugs to construct drug vehicles" into the field of drug formulation and delivery.

2. RESULTS AND DISCUSSIONS

2.1. Morphologies and Sizes. In this study, mono[6-(2-aminoethyleneamino)-6-deoxy]-β-cyclodextrin (ED-β-CD) and PTX were used as the main illustrational experimental materials to explain the strategy. The ED-β-CD/PTX vesicles were prepared by slowly adding drips of PTX ethanol saturated solution into the ED-β-CD aqueous solution. The mixture was sonicated for 30 min, and the resulting solid was filtered away to obtain the vesicular aqueous solution. The vesicular solution exhibited a slightly transparent opalescence, which is totally different from the samples with single compositions. The ED-β-CD aqueous solution exhibited a typical true solution, whereas PTX samples directly dispersed in water would generate obvious cloudy suspension (the white flocculus would easily precipitate if left to stand still for 1 h). Typical Tyndall phenomenon of the ED-β-CD/PTX vesicular solution was detected when a laser pointer (Figure 1) was used to light the sample.

TEM and SEM, as reliable methods for investigating the microassemblies,[34] were employed to observe the morphologies of ED-β-CD/PTX vesicular samples (Figure 2). The TEM result in Figure 2a shows core–shell spheres with obvious contrast between the center and the verge, which is the typical character of vesicular aggregates based on the classical literatures[35,36] and our experience.[37] This kind of morphology by TEM suggests the vesicles are rigid enough to endure the TEM sample preparing process (vesicular solution drips were dried and roasted under an infrared lamp for 30 min) and the electron impact from TEM observing process. SEM images (Figure 2b) further evidence the point. The technique of gold-sputter-coating was applied to the vesicle samples to enhance the conductivity for better observations. Regular 3D spheres were found by SEM visual fields. It should be noted that the vesicle-overlying phenomenon was noticed by both TEM and SEM observations, which may be attributed to the sample concentrating in the drying process for sample-preparing. Vesicles are stacked but not adjoined with each other, not to mention the fusing action, indicating their relatively sturdy colloidal stability. Normally, vesicles assembled by supramolecular amphiphiles are extremely sensitive, both in the mechanical and in thermodynamics stability.[7−11] Owing to the erratic stability, collapsed hollow cavities with color contrast between the gray inners and white surfaces are always found

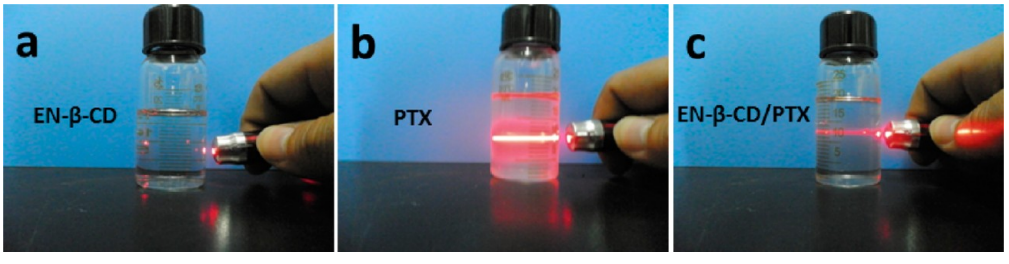

Figure 1. Different phenomenons of the samples [(a) ED-β-CD aqueous solution; (b) PTX dispersed in water; (c) ED-β-CD/PTX vesicular solution] illuminated by a laser pointer.

dx.doi.org/10.1021/jp310261j | J. Phys. Chem. B 2012, 116, 14628−14636

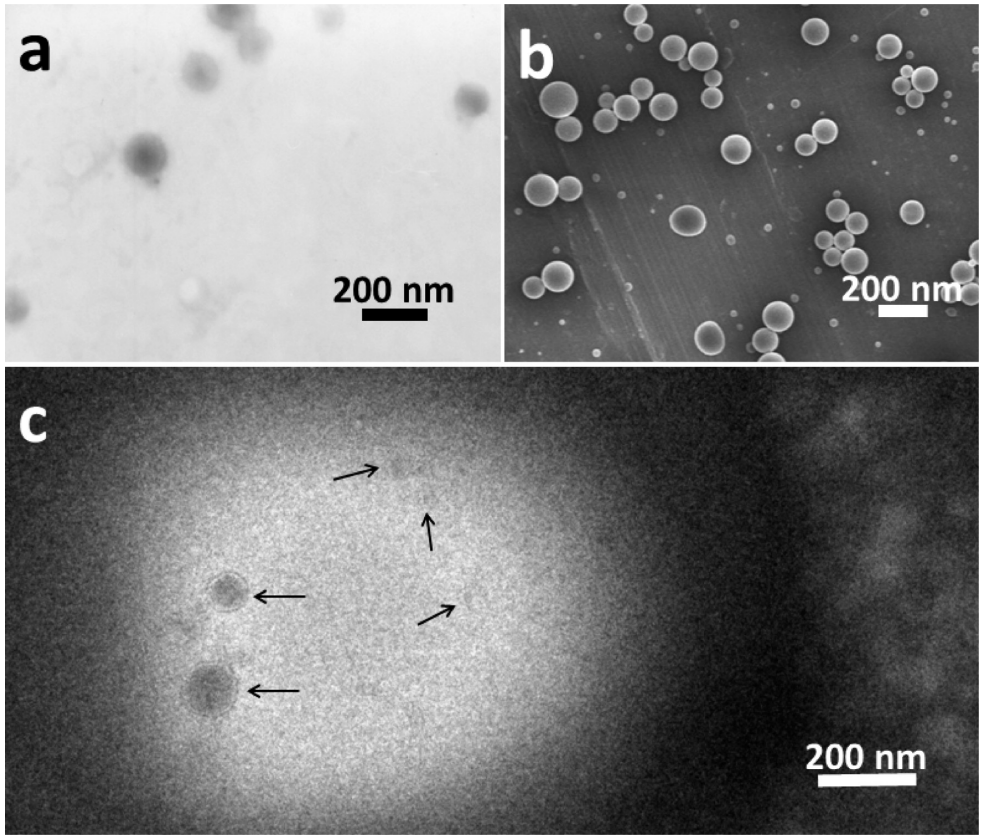

Figure 2. Morphologies of ED-β-CD/PTX vesicular samples by TEM (a), SEM (b), and cryo-TEM (c), scale bars = 200 nm.

when SEM is employed to observe the micro self-aggregates. We just reported an exception of single-layered vesicles formed by supramolecular amphiphiles constructed by specially designed hosts (methyl-modified cyclodextrins) and guest molecules (phthalate esters with double long hydrophobic chains).[17] Even so, a few damaged but 3D spheres with holes notwithstanding could not be avoided. It was unexpected that the ED-β-CD/PTX vesicles can keep even better sphere pattern after the procedures of roasting, vacuum, gold-sputter-coating treatment, and electron impacts. Therefore, we judge that the obtained vesicles are with multilaminar membranes to be capable of maintaining the morphology. To verify the assumption, cryo-TEM, which can directly and wholly reflect the real environmental morphologies of aggregates in solutions, was used to further study the vesicles. Well-defined spheres with layered structures and dark cores were found, as shown in Figure 2c. On the basis of the literatures, they are vesicles with multilaminar membranes.[24,38,39] However, due to the low resolution of the cryo-TEM instrument, only indistinct onion-like structures were recognized. Compared with TEM and SEM vision fields, vesicles are much more scattered by cryo-TEM, possibly because no concentrating process is required in the sample preparation procedure for cryo-TEM observations. Besides, no vesicles were detected in the suspension of sole ED-β-CD or PTX, which revealed the key role of the combination of the supramolecular host and guest in forming the vesicular aggregates.

It cannot be neglected that though the mechanistic property of the ED-β-CD/PTX vesicles is favorable, the thermodynamics stability is not so outstanding. The vesicular aggregations can only last 1 week under room temperature. The ζ potential of the ED-β-CD/PTX vesicle sample was measured to be -22.7 ± 1.3 mV, suggesting the fair thermodynamic stability. After then, some white precipitate would gradually appear that even can be observed by naked eyes. The supernatant solution was detected by TEM and no regular aggregates were found. The precipitate was filtered and proved to be PTX by MS. The stable but short-lived vesicles are still acceptable clinically if the vesicular solution is freshly prepared for the target-carrying applications. These properties may provide new possibilities for the drug or gene loading and releasing in vitro.

The diameters of the obtained spheres are ranged from 50 to 200 nm by all above three means. More precisely, DLS measurement was employed to further measure the particle size distributions (Figure 3), which gave an average hydrodynamic radius (R_h) of 95.5 nm. This means the vesicles' average diameter is 191.0 nm, which is slightly larger than the diameters obtained by TEM, SEM, and cryo-TEM. It is reasonable that

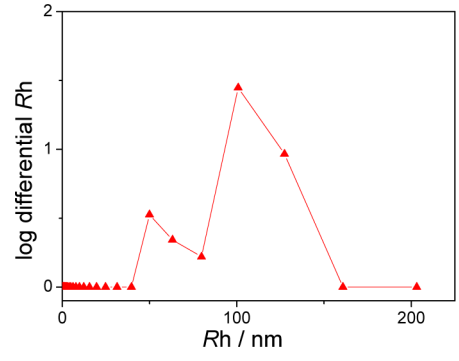

Figure 3. DLS result of the ED-β-CD/PTX vesicles in the aqueous solution at 300 K.

dx.doi.org/10.1021/jp310261j | J. Phys. Chem. B 2012, 116, 14628−14636

TEM, SEM, and cryo-TEM measure the solid spheres, whereas the DLS method measures the swollen spheres.[34] The polydispersity is also in good agreement with the TEM, SEM, and cryo-TEM results.

2.2. Change of the Supramolecular Host Molecules. Monohexanediamine, diethylenetriamine, triethylenetetramine, and tetraethylenepentamine arm modified β-cyclodextrins, which are abbreviated as HD-β-CD, 23-β-CD, 34-β-CD, and 45-β-CD, respectively (Scheme 2), were also tested as the replacement of host molecules and similar results were obtained by TEM observations (Figure 4). The differences between a and d of Figure 4 are probably due to the different extent of phosphotungstic acid staining. Mother β-cyclodextrin (β-CD), hydroxypropyl-β-cyclodextrin (HP-β-CD), sulfobutyl-β-cyclodextrin (SB-β-CD), and methyl-β-cyclodextrin (Me-β-CD) were also tested, no vesicular-formation but only slight PTX-solubilization phenomenon was detected. The comparison suggests the importance of the modified aza-arms, the azyl groups of which can form hydrogen bonds with carbonyl and hydroxyl groups of PTX. Besides the inclusion action, the hydrogen bonds can also strengthen the stability of the supramolecular host–guest complexes. From the ^{1}H NMR spectra of the β-CD/PTX sample in D_2O, few peaks that belong to PTX were found, which further demonstrates the fact that β-CD has poor ability in complexing PTX. All the molecular sizes were simulated, optimized, and calculated by Chemoffice 3D. The data were shown in Scheme 2. It is easy to notice that the sizes of the supramolecular hosts and guest match quite well, which is a basic requirement for the formation of the supramolecular complexes.

Scheme 2. Calculated molecular sizes of the relative guest and host molecules

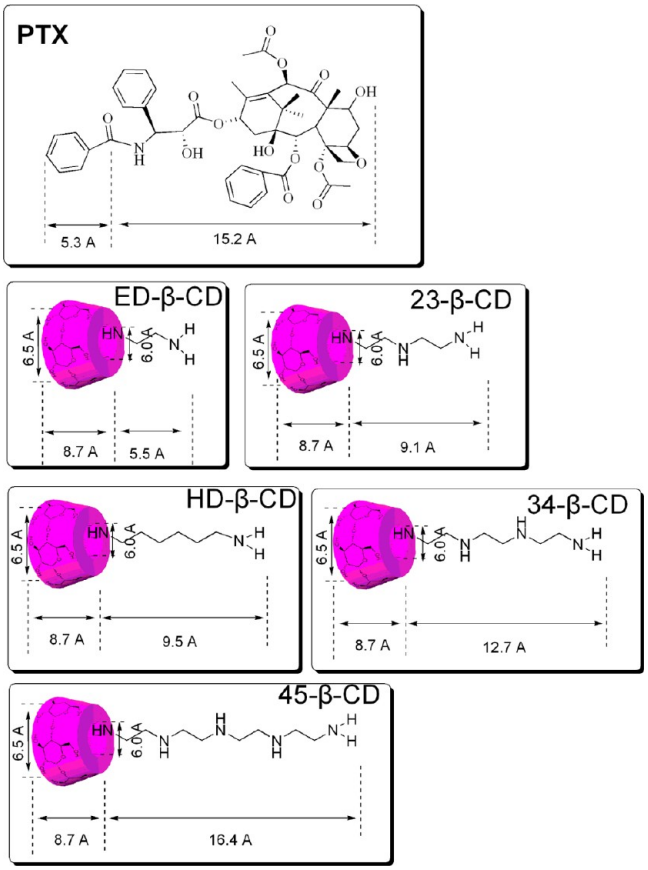

2.3. Change of the Solvent. Alcohols are found to be adverse to this kind of vesicle formation. No vesicles were detected by TEM even when the volume of methanol exceeds 10%. We gradually decreased the methanol amount and finally defined that the vesicular solution containing methanol volume could not reach 4%. Other alcohols, such as ethanol (upper limit 4%), isopropyl alcohol (upper limit 3%), and *n*-butyl alcohol (upper limit 3%) have similar negative effect to vesicles.

Owing to the solvophobic theory,[40] the composition changing of solvents may affect the microstructure in solutions. This may be attributed to two reasons: (i) the single hydrogen-binding site of the alcohols may act as the H-bonds terminator, whereas H-bonds are very crucial in the host–guest combination;[11] (ii) the cyclodextrin cavities may be occupied by these organic solvents, which will exclude the PTX. The correlations between cyclodextrin cavities and PTX were not found in the 2D NMR ROESY spectra (Supporting Information, Figure 4, D_2O/CD_3OD = 5:1, v/v, 300 K), suggesting the decomposition of ED-β-CD and PTX triggered by methanol.

We also tried other seven medias (including phosphate buffered saline (PBS, pH = 7.4), ammonia buffer solution (pH = 7.5), borate buffer solution (pH = 7.3), sodium acetate–acetic acid buffer solution (pH = 4.5), physiological saline (pH = 7.0), *N*-tris(hydroxymethyl) aminomethane–HCl (Tris–HCl, pH = 5.0) buffer solution, and fetal calf serum (FCS, pH = 7.35)), which are commonly used in biological operations (Supporting Information, Figures 6–9). It was found that vesicles can exist in the basic and neutral but not in the acid buffer solutions. By DLS the vesicles' average diameters in PBS buffer, ammonia buffer, borate buffer, and physiological saline are defined as 242.4, 226.3, 168.9, and 224.4 nm, respectively. The TEM and DLS results are in good agreement. Vesicles were also found in FCS, demonstrating their favorable stability in biological tissue fluid and their potential biological applications (Supporting Information, Figure 10).

3. MECHANISM STUDY

3.1. FT-IR Characterizations. FT-IR is widely used in studying the molecular interactions in material science.[41] The ED-β-CD/PTX solid sample was isolated by freeze-drying the ED-β-CD/PTX vesicular solution. The FT-IR spectral comparison of PTX, ED-β-CD, their physical mixture, and the supramolecular complex was undertaken (Figure 5). Both of the characteristic peaks of PTX (the green dotted lines, $\nu_{C=O}$, 1724 cm^{-1}; ν^{as}_{C-O-C}, 1254 cm^{-1}) can be found in the spectra of the physical mixture and supramolecular complex, showing the existence of PTX in them. Meanwhile, the characteristic peaks of ED-β-CD (the red dotted lines, ν_{C-N}, 1159 cm^{-1}; ρ_{CH_2}, 579 cm^{-1}) can also be found in the resulting spectra. On the other hand, the intensity of $\nu_{C=O}$ and ν^{as}_{C-O-C} peaks of PTX changed greatly in the complex spectrum compared with the physical mixture. The ν_{O-H} peak (3366 cm^{-1} → 3384 cm^{-1}), ν_{C-N} peak (1159 cm^{-1} → 1155 cm^{-1}), and δ_{N-H} peak (706 cm^{-1} → 710 cm^{-1}) also show shifts after comparing the spectra of ED-β-CD and ED-β-CD/PTX complex, suggesting the hydrogen bonds formed between host and guest molecules participated by the amine groups in the aza-arm. It is easy to recognize the spectrum of the physical mixture as the simple overlying of ED-β-CD and PTX spectra.

dx.doi.org/10.1021/jp310261j | J. Phys. Chem. B 2012, 116, 14628–14636

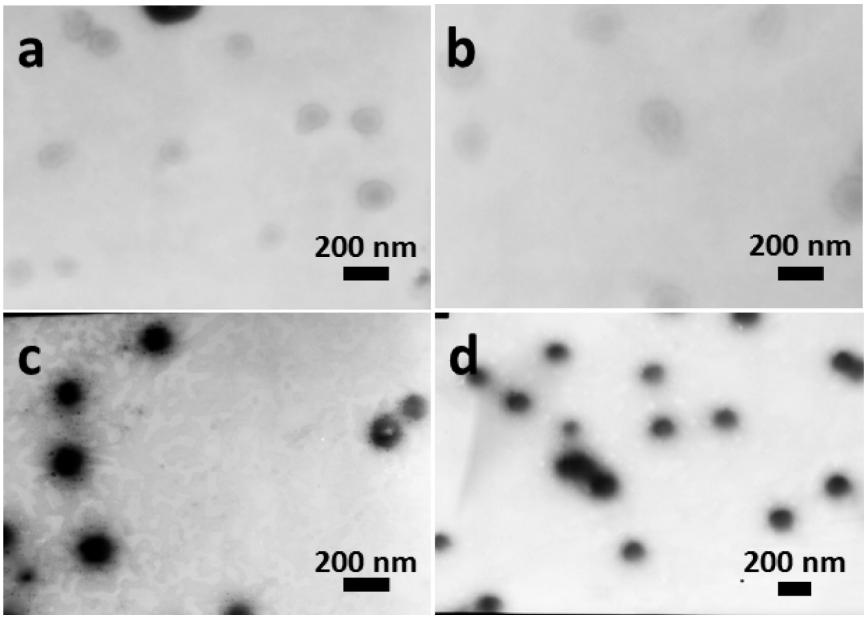

Figure 4. Morphologies of the vesicular samples by TEM (a) HD-β-CD/PTX, (b) 23-β-CD/PTX, (c) 34-β-CD/PTX, and (d) 45-β-CD/PTX, scale bars = 200 nm.

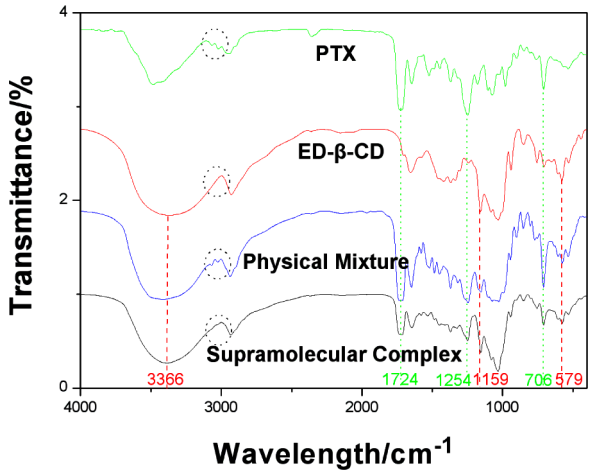

Figure 5. FT-IR spectra comparison of PTX, ED-β-CD, their physical mixture and supramolecular complex.

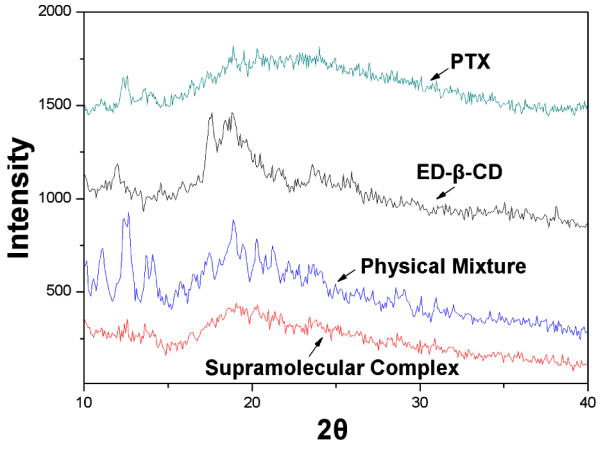

Figure 6. XRD spectra comparison of PTX, ED-β-CD, their physical mixture, and supramolecular complex.

And the spectrum of the supramolecular complex shows obvious differences from the physical mixture's, especially in the peaks among 3000 cm^{-1} (the circled peaks). Besides, the stretching vibration peaks of the hydroxyl group appearing in the wavelength of 3360 cm^{-1} are obviously different both in shape and in intensity, also meaning the newly formed hydrogen bonds in the complex.[41,42]

3.2. XRD Characterizations. XRD, as a powerful method in analyzing species in supramolecular materials,[43,44] was used to study the mechanism (Figure 6). Characteristic peaks around $2\theta = 13°$ of PTX were found both in the physical mixture and in the supramolecular complex (though very weak diffractions), proving the existence of PTX in them. However, the physical mixture is obviously an overlying of ED-β-CD and PTX, whereas the ED-β-CD/PTX complex is more like in an amorphous state. The results suggest that in the complex, PTX molecules exist in an independent condition, possibly complexed by ED-β-CD.

3.3. Thermal Analysis. The thermal analysis, including thermogravimetric analysis (TGA) and differential scanning calorimetry (DSC), of PTX, ED-β-CD, their physical mixture, and the supramolecular complex was carried out. The TGA curves belonging to the physical mixture and supramolecular complex are close but show obvious differences, both in peaks and in shape (Figure 7). Furthermore, the DSC thermogram gives more information about the thermal properties. The physical mixture shows an exothermic peak at 206 °C, whereas the supramolecular complex shows an endothermic peak at 203 °C. Considering the physical mixture and supramolecular complex are with the same chemical compositions, their obviously different TGA and DSC curves suggest the existence of host−guest interactions in the supramolecular complex.

3.4. NMR Characterizations. ^{1}H NMR, as one of the most precise and reliable methods in detecting the molecular interactions in solutions, was employed to further study the mechanism.[45] From the comparison of ^{1}H NMR results of ED-β-CD and ED-β-CD/PTX samples (Table 1, the original spectra are included in Supporting Information). It is known

dx.doi.org/10.1021/jp310261j | J. Phys. Chem. B 2012, 116, 14628−14636

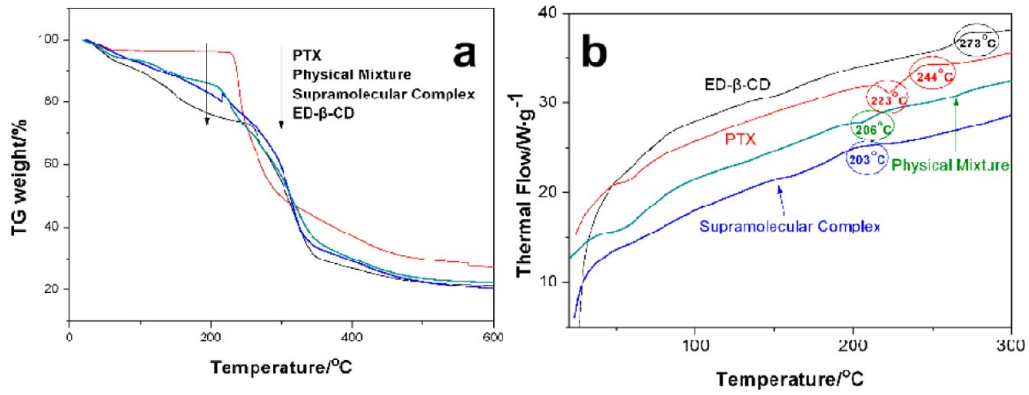

Figure 7. TGA (a) and DSC (b) spectra comparisons of PTX, ED-β-CD, their physical mixture, and supramolecular complex.

Table 1. ^{1}H NMR Comparison of the Chemical Shifts of Single ED-β-CD and ED-β-CD/PTX[a]

entry	H1	H3	H5	H6	H2	H4
δ(ED-β-CD)	5.008	3.903	3.818	3.788	3.587	3.521
δ(ED-β-CD/PTX)	5.005	3.880	3.807	3.766	3.583	3.513
$\Delta\delta^b$	0.005	0.023	0.011	0.022	0.004	0.008

[a]DHO peak (δ = 4.699) is as the interior label. [b]$\Delta\delta$ = δ(ED-β-CD)-δ(ED-β-CD/PTX).

that H2 and H4 protons are located outside the cyclodextrin cavity, while H3 and H5 protons are located inside the cavity.[18] From the table, it is easy to find out that both H3 and H5 protons exhibit significantly larger chemical shifts than the H1, H2, and H4 proton, which means that PTX is included in the cyclodextrin cavity. It also should be noted that H6 proton existing on the primary face shows an obvious chemical shift, suggesting the rest excluded moiety of PTX remains outside the cavity, participating with the aza-arm.

2D NMR ROESY is a powerful tool in detecting pairs of nuclei that are close in space (smaller than 5 Å), even if they are noncovalently bound.[46] Clear correlations between H protons (δ = 7.5 ppm, benzene ring A of PTX) and H3 and H5 (locating inside the cavity of ED-β-CD) were found in the 2D NMR ROESY spectra of ED-β-CD/PTX sample in D_2O, which strongly demonstrates the entrance of PTX into the ED-β-CD cavity.

It is known that the solubility of PTX is as low as 4.03 μg/mL in water,[47] which makes it always attractive by transferring PTX into aqueous solution for the bioavailability. NMR is almost blind to PTX when D_2O is the solvent.[48] The ^{1}H NMR analysis of saturated ED-β-CD/PTX D_2O solution was undertaken. Clear peaks belonging to PTX can be seen in the ED-β-CD/PTX ^{1}H NMR spectrum, evidencing the crucial role that ED-β-CD plays. On the basis of calculating the ratio of the integral areas respectively belonging to ED-β-CD and PTX, we obtained the molecular ratio is about 5:2, from which the maximal solubility is calculated as 0.34 mg/mL. The PTX solubility in the ED-β-CD/PTX vesicle system is almost 80 times as high as the sole PTX in water. Meanwhile, the existence of free ED-β-CD without trapping PTX cannot be neglected in the aqueous solution.

Liu reported that double-cyclodextrin bridged by polyethyleneamines $(-(CH_2)_2-NH-)_n$ have favorable capability in encapsulating PTX in a 1:2 mode.[48] It is believed that the space between bridged cyclodextrins can be considered as "expanded space" and can provide more possibility for including relatively "large" guest molecules. Similarly, ED-β-CD, HD-β-CD, 23-β-CD, 34-β-CD, and 45-β-CD can also be regarded to have the "expanded space" with variable volumes between the modified arms and the cyclodextrin moieties, which could be applied to better encapsulate the nonincluded part of PTX.

Cyclodextrins, with hydrophobic inner cavities and hydrophilic rims, have the capability to bind certain substrates to form inclusion complexes.[48] From the experimental results and the above analysis, we assume that the benzene ring A of the PTX molecule enters the cyclodextrin cavity through the primary face, while the rest moiety bearing carbonyl and hydroxyl groups will remain outside the cavity, participating with the aza-arm by hydrogen bonds. Thus, the supramolecular complex forms a distinctive kind of "amphiphile", in which the cyclodextrin moiety plays a role as the "hydrophilic head", while the PTX moiety is the "hydrophobic tail". It can be concluded that the supramolecular combination of the host and guest molecules plays the fundamental role in constructing the amphiphile. While being ultrasonicated and homogeneously dispersed into water, the peculiar "supramolecular amphiphiles" can self-assemble into vesicular aggregates. The hydrophilic heads (cyclodextrins) interact favorably with the surrounding water, while the hydrophobic tails (PTX) minimize their exposure to water by aggregating together. The proposed mechanism is illustrated in Scheme 3.

4. RESPONSE TO Cu^{2+}

By TEM observations, ED-β-CD/PTX, HD-β-CD/PTX, 23-β-CD/PTX, 34-β-CD/PTX, and 45-β-CD/PTX vesicles will disappear upon the addition of Cu^{2+} ions. Meanwhile, some crystalline-like solid was found in the TEM visual fields (see

Scheme 3. Proposed Vesicle-Formation Mechanism

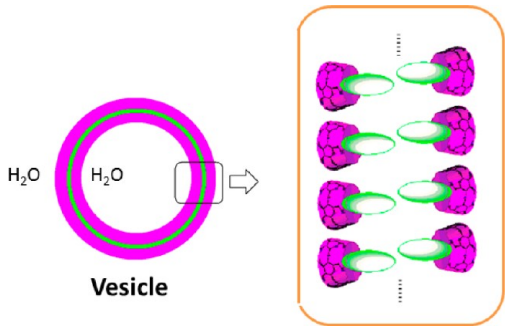

dx.doi.org/10.1021/jp310261j | J. Phys. Chem. B 2012, 116, 14628−14636

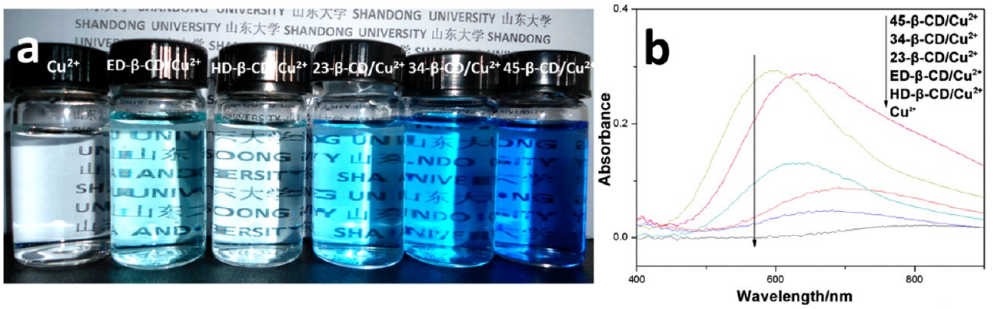

Figure 8. (a) Photographs and (b) UV−vis absorbance of the filtered samples of Cu^{2+}, ED-β-CD/PTX/Cu^{2+}, HD-β-CD/PTX/Cu^{2+}, 23-β-CD/PTX/Cu^{2+}, 34-β-CD/PTX/Cu^{2+}, and 45-β-CD/PTX/Cu^{2+}. The cyclodextrin concentration was 10^{-3} mol/L, and the concentration of Cu^{2+} was set as 2×10^{-3} mol/L).

Supporting Information). The suspension was filtered through a 0.45 μm filter membrane to obtain some white solid, which was proved to be PTX by MS characterization.

It is interesting that as the *N* atom number of the host arm increases, the filtrate's color becomes increasingly deep (Figure 8). This phenomenon proves the coordination of the host's arm with the Cu^{2+} ion,[49] which is comparable with the reaction of EDTA or NH_3 with Cu^{2+}. It also should be pointed out that with the same number of *N* atoms, the HD-β-CD/Cu^{2+} filtrate's color is lighter than that of ED-β-CD/Cu^{2+}, which may be ascribed to the longer distance between the *N* atoms of HD-β-CD arm. The UV−vis absorbance spectra further demonstrate the assumption. Both the shape and the intensity of the absorbance peaks change greatly as the β-CD derivate differs. New UV absorbance peaks are ascribed to the metal−ligand charge transfer process. Meanwhile, β-CD/Cu^{2+}, HP-β-CD/Cu^{2+}, SB-β-CD/Cu^{2+}, and Me-β-CD/Cu^{2+} show no noticeably different color change compared with the sole aqueous Cu^{2+} solution (for the pictures, please see Supporting Information), suggesting probably no coordination phenomenon occurs. Due to the paramagnetism of Cu^{2+}, it is difficult to use NMR to observe the environmental states of the samples containing copper.[50]

Liu[48] reported that once the double cyclodextrins bridged by polyethyleneamines (−$(CH_2)_2$−NH−) coordinate with Cu^{2+} ions, the "expanded space" for the guest will be greatly reduced. We indicate that *N* atoms of ED-β-CD molecules will coordinate with the introduced Cu^{2+} ions, possibly decreasing the space for the inclusion. The hydrogen bonds between host−guest will also be weakened as the coordinate with Cu^{2+}. Both of them will drives the PTX molecules out from the supramolecular complex (Scheme 4). The study will provide a novel method to carry and controlled-release PTX drugs. Considering the prevalent species containing copper in vivo (such as cytochrome C oxidase,[51] superoxide dismutase,[52] tyrosinase, etc.), our study will be of potential application in designing novel targeting drug-carrying biomaterials.

Scheme 4. PTX Release Process Triggered by Adding Cu^{2+}

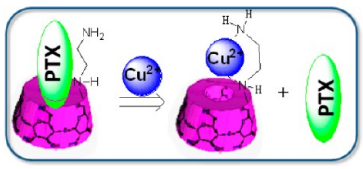

5. CONCLUSION

In this study, we propose a novel strategy for constructing vesicles from peculiar supramolecular amphiphiles. PTX can be straightforwardly used as partial building blocks for the vesicles. The vesicles were fully characterized by TEM, SEM, cryo-TEM, and DLS, and the mechanism was also suggested on the basis of the ^{1}H NMR, 2D NMR ROESY, FT-IR, XRD, and thermal analysis results. The effects of the change of the host molecule and the solvent to the vesicular formation were also studied. The introduction of Cu^{2+} will vanish the vesicles, as well as drive PTX out of the supramolecular complex. Considering cyclodextrins and their derivates are with favorable biocompatibility, we believe the study will provide more practical possibilities for the clinically anticancer applications. This research may also cast a new light to the area of design and preparation of efficient drug-carrying vehicles.

6. EXPERIMENTAL SECTION

6.1. Materials. β-CD, ED-β-CD, HD-β-CD, 23-β-CD, 34-β-CD, 45-β-CD, HP-β-CD, SB-β-CD, and Me-β-CD were purchased from Binzhou Zhiyuan Biotechnology Co. Ltd., China, and dried under vacuum for 12 h at 50 °C before using. ED-β-CD, HD-β-CD, 23-β-CD, 34-β-CD, and 45-β-CD are mono-6-deoxy-substituted. The synthesis method is according to the literature,[37,53] and the substitution degree is defined to be 1. HP-β-CD has an n = 4.5 substitution degree, whereas SB-β-CD has an n = 6.9 substitution degree. The substituted positions of HP-β-CD and SB-β-CD are not definite. Me-β-CD (heptapkis (2,6-di-*O*-methyl)-β-CD cyclodextrin) has an n = 7.9 substituting degree. PTX was purchased from Beijing Noezer Pharmaceutical Co. Ltd., China. PBS (pH = 7.4) buffer was prepared by adding 8 g of NaCl, 2.9 g of $Na_2HPO_4 \cdot 12H_2O$, 0.2 g of KCl, and 0.2 g of KH_2PO_4 into 1000 mL of distilled water, and then the mixture was sonicated for 20 min at 300 K. Ammonia buffer solution (pH = 7.5) was prepared by adding 2.8 mL of $NH_3 \cdot H_2O$ (15 mol/L) and 120 g of NH_4Cl into 1000 mL of distilled water, and then the mixture was sonicated for 20 min at 300 K. Borate buffer solution (pH = 7.3) was prepared by 1.0 g of $Na_2B_4O_7 \cdot 12H_2O$, 11.1 g of H_2BO_3, and 2.6 g of NaCl in 1000 mL of distilled water and then the mixture was sonicated for 20 min at 300 K. Physiological saline (pH = 7.0) was prepared by adding 0.9 g of NaCl into 100 mL of distilled water and then the mixture was sonicated for 20 min at 300 K. FCS (pH = 7.35, with low esotoxin and without mycoplasma or bacteriophage) was purchased from Zhejiang Tianhang Biotech. Co., Ltd., China. Sodium acetate−acetic acid buffer solution, pH = 4.5, was prepared by adding 18 g

dx.doi.org/10.1021/jp310261j | J. Phys. Chem. B 2012, 116, 14628−14636

CH_3COONa and 98 mL CH_3COOH into 1000 mL distilled water and then sonicated for 20 min at 300 K. Tris−HCl buffer solution, pH = 5.0, was purchased from Shanghai Zhongkun Biotech. Co., Ltd., China. All other organic reagents were of analytical purity and used as received without further purification.

6.2. Analytical Measurements and Methods. All samples for TEM were prepared via the phosphotungstic acid staining technique. The JEM-100CX electron microscope (http://www.jeol.com/) was employed. SEM images were obtained with a Hitachi S-4800 scanning electron microscope by coating the vesicular solution to the base plate and then dried and sputter-coated with gold. DLS measurements were carried out with a Wyatt QELS Technology DAWN HELEOS instrument poised at constant room temperature (25 °C) by using a 12-angle replaced detector in a scintillation vial and a 50 mW solid-state laser (λ = 658.0 nm). All solutions for DLS were filtered through a 0.45 μm filter membrane before detection. 2D NMR ROESY experiments were recorded using an INOVA-600 (600 MHz) spectrometer at ambient temperature, with a mixing time of 0.200 s, a relaxation delay time of 1.000 s, and an acquisition time of 0.228 s. UV−vis spectra were recorded at room temperature with a TU-1800pc UV−vis spectrophotometer. All pulse sequences were set according to the company standards. The electrophoretic measurement for the zeta potential was performed on JS94J apparatus equipped with a flow-through cell (Powereach, China). Mass spectroscopy (MS) was run on a 6510 Q-TOF MS instrument from Agilent Technologies Co. The solutions containing different IR spectra were obtained on an Avatar 370 FT-IR spectrometer. XRD experiments were performed on a German Bruker/D8 ADVANCE diffractometer with Cu Kα radiation (λ = 0.154 06 nm, 40 kV, 40 mA) in a reflectance mode and a graphite monochromator at ambient temperature. The sample holder is a HF-corroded glass sheet. A DSC 822e thermal analysis system from Mettler-Toledo (Swiss) was employed. The samples (about 3 mg) were weighed into unsealed aluminum pans. The DSC thermogram was recorded with the temperature ranging from 25 to 800 °C at the heating rate of 10 °C/min under a N_2 atmosphere with the reference of empty aluminum. Chem 3D simulation and calculation were performed in ChemOffice Ultra 8.03 version from Cambridge Company, USA. The sonication was performed with a KQ116 ultrasonic cleaner for jewelry, Kunshan ultrasonic apparatus Co. Ltd., China. The laser pointer (3 W) for the Tyndall phenomenon was from Yingkailai Co. Ltd., China.

6.3. Preparation of the Vesicles and Samples for Characterizations. The ED-β-CD mother aqueous solution (10^{-2} mol/L) was prepared by adding a certain amount of ED-β-CD powder into water and the obtained mixture was then sonicated for 30 min. The ED-β-CD aqueous solution (10^{-3} mol/L, also for the test of the Tyndall phenomenon) was prepared by simply diluting the mother solution. A certain volume of PTX ethanol saturated solution was added into the ED-β-CD aqueous solution (10^{-3} mol/L), and the mixture was sonicated for 30 min. The solids was filtered through a 450 nm filter membrane to obtain the ED-β-CD/PTX vesicular aqueous solution. The ethanol volume ratio is 1.9%, which is lower than the upper limit (4%, by volume) of the vesicles' tolerance level for ethanol. If necessary, the MWCO2000 dialysis bag or freeze-drying method can be employed to remove the organic solvents. The filtered solid was proved to be PTX by MS characterization. No filtering method was employed for the vesicles in fetal calf serum (FCS). The sample of PTX dispersed in water for the test of Tyndall phenomenon was prepared by dripping the same amount as below into water and the obtained suspension was then sonicated for 30 min. The experiments of the response to Cu^{2+} were carried out by directly adding a certain amount of 0.1 mol/L $CuCl_2$ aqueous solution (0.1 mol/L) into the freshly prepared vesicular solution, which was then sonicated for 30 min. The samples for the NMR characterizations were prepared by adding certain amount of ED-β-CD/PTX (1:1, by mol) powders into D_2O and followed by filtering. Vesicle samples for TEM characterization were obtained by dripping the vesicular solution to the copper grids, which were then dried under the infrared lamp. Phosphotungstic acid solution as the staining agent was dripped to the copper grid. The obtained stained vesicle sample was then dried under the infrared lamp again for 30 min. TEM experimental results were adopted at least when 3 in 4 times were with the same results. SEM samples were directly treated from the TEM samples.

6.4. Preparation of the ED-β-CD/PTX Solid Complex and Their Physical Mixture. The ED-β-CD/PTX solid complex for FT-IR, XRD, and thermal analysis characterizations were isolated by freeze-drying the ED-β-CD/PTX aqueous vesicular solution. The ED-β-CD/PTX physical mixture was prepared by simply mixing ED-β-CD and PTX together with the same molar ration as the complex. The mixture should be freshly prepared to avoid the possible complexing during the placed period. It should be noted that the physical mixture sample of ED-β-CD/PTX for FT-IR characterization was prepared as follows: ED-β-CD or PTX powders should be ground with dry KBr separately, mixed together, and tableted into a cake, to avoid the possible inclusion between ED-β-CD and PTX during the grinding procedure.[54,55] Additionally, the sizes of the PTX solid particles are much larger than the ED-β-CD powder solid. Thus, during the XRD samples preparation, the ED-β-CD will easily sink to the bottom of the glass cave. This may be why the peaks of PTX seem stronger than ED-β-CD's in the XRD spectrum of the physical mixture.

■ ASSOCIATED CONTENT

Supporting Information

(1) NMR spectrum of ED-β-CD/PTX in D_2O at 300 K; (2) photograph of the β-CD/Cu^{2+}, HP-β-CD/Cu^{2+}, SB-β-CD/Cu^{2+}, and Me-β-CD/Cu^{2+} samples; (3) loading rate of PTX; (4) morphologies in other medias; (5) TEM images of ED-β-CD/PTX samples treated by Cu^{2+}. This information is available free of charge via the Internet at http://pubs.acs.org.

■ AUTHOR INFORMATION

Corresponding Author

*Tel.: +86-531-88363306. Fax: +86-531-88564464. E-mail: haoay@sdu.edu.cn.

Notes

The authors declare no competing financial interest.

■ ACKNOWLEDGMENTS

This work was supported by the NSFC (Grant No. 20625307), National Basic Research Program of China (973 Program, 2009CB930103), Shandong Province Natural Science Foundation (No. ZR2009CL022), and Graduate Independent Innovation Foundation of Shandong University (GIIFSDU, yzc09057). T.S. thanks the Chinese Scholarship Council (CSC)

for providing financial support during his stay at École Normale Supérieure (ENS), Paris. T.S. greatly thanks Dr. Prof. Ludovic Jullien from École Normale Supérieure, Paris for the scientific culture.

REFERENCES

(1) Tomatsu, I.; Hashidzume, A.; Harada, A. *Macromolecules* **2005**, *38*, 5223−5227.
(2) Beck, J. B.; Rowan, S. J. *J. Am. Chem. Soc.* **2003**, *125* (46), 13922−13923.
(3) Sun, T.; Li, Y.; Zhang, H.; Li, J.; Xin, F.; Kong, L.; Hao, A. *Colloids Surf. A* **2011**, *375*, 87−96.
(4) Sun, T.; Zhang, H.; Yan, H.; Li, J.; Cheng, G.; Hao, A.; Qiao, H.; Xin, F. *Supramol. Chem.* **2011**, *23*, 351−364.
(5) Zhang, H.; Xin, F.; An, W.; Hao, A.; Wang, X.; Zhao, X.; Liu, Z.; Sun, L. *Colloids Surf. A* **2010**, *363*, 78−85.
(6) Sun, L.; Zhang, H.; An, W.; Hao, A.; Hao, J. *J. Inclusion Phenom. Macrocyclic Chem.* **2010**, *68*, 277−285.
(7) Zhang, H.; Liu, Z.; Xin, F.; An, W.; Hao, A.; Li, J.; Li, Y.; Sun, L.; Sun, T.; Zhao, W.; Li, Y.; Kong, L. *Carbohydr. Res.* **2011**, *346*, 294−304.
(8) An, W.; Zhang, H.; Sun, L.; Hao, A.; Hao, J.; Xin, F. *Carbohydr. Res.* **2010**, *345*, 914−921.
(9) Zhang, H.; Shen, J.; Liu, Z.; Bai, Y.; An, W.; Hao, A. *Carbohydr. Res.* **2009**, *344*, 2028−2035.
(10) Zhang, H.; An, W.; Liu, Z.; Hao, A.; Hao, J.; Shen, J.; Zhao, X.; Sun, H.; Sun, L. *Carbohydr. Res.* **2010**, *345*, 87−96.
(11) Zhang, H.; Shen, J.; Liu, Z.; Hao, A.; Bai, Yan.; An, W. *Supramol. Chem.* **2010**, *22* (5), 297−310.
(12) Luo, C.; Zuo, F.; Zheng, Z.; Cheng, X.; Ding, X.; Peng, Y. *Macromol. Rapid Commun.* **2008**, *29*, 149−154.
(13) Zou, J.; Tao, F.; Jiang, M. *Langmuir* **2007**, *23*, 12791−12794.
(14) Wang, Y.; Ma, N.; Wang, Z.; Zhang, X. *Angew. Chem., Int. Ed.* **2007**, *46*, 2823−2826.
(15) Zou, J.; Guan, B.; Liao, X.; Jiang, M.; Tao, F. *Macromolecules* **2009**, *42*, 7465−7473.
(16) Jin, Q.; Liu, G.; Liu, X.; Ji, J. *Soft Matter* **2010**, *6*, 5589−5595.
(17) Sun, T.; Shen, J.; Yan, H.; Hao, J.; Hao, A. *Colloids Surf. A* **2012**, *414*, 41−49.
(18) Xin, F.; Zhang, H.; An, W.; Sun, L.; Hao, A.; Li, Y. *J. Dispersion Sci. Technol.* **2012**, *33*, 1−4.
(19) Zhang, H.; Li, Y.; Sun, H.; Xin, F.; Liu, Z.; Hao, A.; Li, J.; Shen, J.; Xu, S.; An, W.; Sun, L.; Sun, T.; Zhao, W.; Li, Y.; Kong, L. *J. Dispersion Sci. Technol.* **2011**, *32*, 834−839.
(20) Zhang, H.; Sun, L.; Liu, Z.; An, W.; Hao, A.; Xin, F.; Shen, J. *Colloids Surf. A* **2010**, *358*, 115−121.
(21) Liu, Y.; Wang, K. R.; Guo, D. S.; Jiang, B. P. *Adv. Funct. Mater.* **2009**, *19*, 2230−2235.
(22) Eelkema, R.; Maeda, K.; Odell, B.; Anderson, H. L. *J. Am. Chem. Soc.* **2007**, *129*, 12384−12385.
(23) Li, S.; Taura, D.; Hashidzume, K.; Harada, A. *Chem. Asian. J.* **2010**, *5*, 2281−2289.
(24) Gao, Y.; Hao, J. *J. Phys. Chem. B* **2009**, *113*, 9461−9471.
(25) Allen, T. M.; Cullis, P. R. *Science* **2004**, *303*, 1818−1822.
(26) Zhang, X.; Wang, C. *Chem. Soc. Rev.* **2011**, *40*, 94−101.
(27) Xiao, K.; Luo, J.; Fowler, W. L.; Li, Y.; Lee, J. S.; Xing, L.; Cheng, R. H.; Wang, L.; Lam, K. S. *Biomaterials* **2009**, *30*, 6006−6016.
(28) Danhier, F.; Lecouturier, N.; Vroman, B.; Jérome, C.; Marchand-Brynaert, J.; Feron, O.; Préat, V. *J. Controlled Release* **2009**, *133*, 11−17.
(29) Yu, D.; Lu, Q.; Xie, J.; Fang, C.; Chen, H. *Biomaterials* **2010**, *31*, 2278−2292.
(30) Sun, T.; Guo, Q.; Zhang, C.; Hao, J.; Xing, P.; Su, J.; Li, S.; Hao, A.; Liu, G. *Langmuir* **2012**, *28*, 8625−8636.
(31) Matsumura, Y.; Maeda, H. *Cancer Res.* **1986**, *46* (12), 6387−6392.
(32) Tu, C.; Zhu, L.; Li, P.; Chen, Y.; Su, Y.; Yan, D.; Zhu, X.; Zhou, G. *Chem. Commun.* **2011**, *47*, 6063−6065.
(33) Szejtli, J. *Chem. Rev.* **1998**, *98*, 1743−1754.
(34) Maurice, R.; Eftink, M. L.; Bystrom, K.; Perlmutter, H. D.; Kristol, D. S. *J. Am. Chem. Soc.* **1989**, *111*, 6765−6772.
(35) Wang, L.; Liu, H.; Hao, J. *Chem. Commun.* **2009**, *135*, 1353−1355.
(36) Yin, H.; Lei, S.; Zhu, S.; Huang, J.; Ye, J. *Chem.—Eur. J.* **2006**, *12*, 2825−2835.
(37) Sun, T.; Zhang, H.; Kong, L.; Qiao, H.; Li, Y.; Xin, F.; Hao, A. *Carbohydr. Res.* **2011**, *346*, 285−293.
(38) Zhou, X.; Dong, S.; Hao, J. *Colloid Polym. Sci.* **2011**, *289*, 1451−1457.
(39) Wang, D.; Dong, R.; Long, P.; Hao, J. *Soft Matter* **2011**, *7*, 10713−10719.
(40) Ray, A. *Nature* **1971**, *231*, 313−315.
(41) Li, G.; McGown, L. B. *Science* **1994**, *264*, 249−251.
(42) Sun, T.; Zhao, W.; Hao, A.; Sun, L. *Synth. Commun.* **2011**, *41*, 3097−3105.
(43) Kong, L.; Sun, T.; Xin, F.; Zhao, W.; Zhang, H.; Li, Z.; Li, Y.; Hou, Y.; Li, S.; Hao, A. *Colloids Surf. A* **2011**, *392*, 156−162.
(44) Li, Y.; Liu, J.; Du, G.; Yan, H.; Wang, H.; Zhang, H.; An, W.; Zhao, W.; Sun, T.; Xin, F.; Kong, L.; Li, Y.; Hao, A.; Hao, J. *J. Phys. Chem. B* **2010**, *114* (32), 10321−10326.
(45) Schneider, H. J.; Hacket, F.; Rüdiger, V. *Chem. Rev.* **1998**, *98*, 1755−1785.
(46) Hu, S.; Li, J.; Xiang, J.; Pan, J.; Luo, S.; Cheng, J. *J. Am. Chem. Soc.* **2010**, *132* (20), 7216−7228.
(47) Liang, L.; Lin, S.; Dai, W.; Lu, J.; Yang, T.; Xiang, Y.; Zhang, Y.; Li, R.; Zhang, Q. *J. Controlled Release* **2012**, *160*, 618−629.
(48) Liu, Y.; Chen, G. S.; Chen, Y.; Cao, D. X.; Ge, Z. Q.; Yuan, Y. J. *Bioorg. Med. Chem.* **2004**, *12*, 5767−5775.
(49) Masakatsu, S.; Motomu, K. *Chem. Rev.* **2008**, *108*, 2853−2873.
(50) Małeckia, J. G.; Groń b, T.; Dudab, H. *Polyhedron* **2012**, *36* (1), 56−68.
(51) Corpas, F. J.; Fernández-Ocaña, A.; Carreras, A.; Valderrama, R.; Luque, F.; Esteban, F. J.; Rodríguez-Serrano, M.; Chaki, M.; Pedrajas, J. R.; Sandalio, L. M.; del Río, L. A.; Barroso, J. B. *Plant Cell Physiol.* **2006**, *47* (7), 984−994.
(52) Tsukihara, T.; Aoyama, H.; Yamashita, E.; Tomizaki, T.; Yamaguchi, H.; Shinzawa-Itoh, K.; Nakashima, R.; Yaono, R.; Yoshikawa, S. *Science* **1995**, *269*, 1069−1074.
(53) Brady, B.; Lynam, N.; O'Sullivan, T.; Ahern, C.; Darcy, R. *Org. Synth.* **2004**, *10*, 686.
(54) Takahashi, K. *Chem. Rev.* **1998**, *98*, 2013−2033.
(55) Uekama, K.; Hirayama, F.; Irie, T. *Chem. Rev.* **1998**, *98*, 2045−2076.